

# Lithiation of Prochiral 2,2'-Dichloro-5,5'-dibromo-4,4'-bipyridine as a Tool for the Synthesis of Chiral Polyhalogenated 4,4'-Bipyridines

Victor Mamane,<sup>\*,†</sup> Emmanuel Aubert,<sup>‡</sup> Paola Peluso,<sup>§</sup> and Sergio Cossu<sup>||</sup>

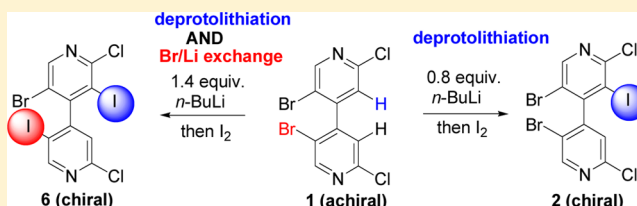
<sup>†</sup>Laboratoire SRS MC UMR CNRS 7565 and <sup>‡</sup>Laboratoire CRM2 UMR CNRS 7036, Université de Lorraine, 54506 Vandoeuvre-les-Nancy, France

<sup>§</sup>Istituto di Chimica Biomolecolare ICB CNR, UOS di Sassari, 07100 Sassari, Italy

<sup>||</sup>Dipartimento di Scienze Molecolari e Nanosistemi, Università Ca' Foscari di Venezia, 30123 Venezia, Italy

**S** Supporting Information

**ABSTRACT:** Lithiation of the achiral tetrahalogenated 4,4'-bipyridine **1** with alkylolithiums was investigated. *n*-BuLi was found to induce either the chlorine-directed deprotolithiation reaction alone or with a concomitant halogen–lithium exchange furnishing after iodine trapping chiral 4,4'-bipyridines **2** and **6**, respectively. The role of *n*-BuLi in the deprotolithiation process of **1** was elucidated on the basis of isolated secondary derivatives. After deprotolithiation, the lithiated species could be trapped by different electrophiles such as MeI, TMSCl, MeSSMe, R<sub>3</sub>SnCl (R = Me or *n*-Bu), and PPh<sub>2</sub>Cl. Moreover, 4,4'-bipyridine **2** was submitted to cross-coupling reactions (Suzuki and Sonogashira) which occurred selectively at the carbon–iodine bond. All compounds of this new family of atropisomeric 4,4'-bipyridines were separated by chiral HPLC (high-performance liquid chromatography), and the absolute configurations of obtained enantiomers were mainly assigned by XRD (X-ray diffraction) using anomalous dispersion.



## INTRODUCTION

The 4,4'-bipyridine framework represents an important synthetic intermediate for the preparation of viologens,<sup>1</sup> liquid crystals,<sup>2,3</sup> and polyheterocyclic compounds<sup>4,5</sup> and can serve as a target for biological systems.<sup>6,7</sup> More importantly, 4,4'-bipyridine ligands play a key role in the design of metal organic frameworks (MOFs),<sup>8</sup> which represent promising nano- or microporous materials with various potential applications.<sup>9</sup> Specifically, homochiral MOFs have found some applications in enantioselective separation<sup>10</sup> and heterogeneous asymmetric catalysis.<sup>11,12</sup> Among the different routes to prepare homochiral MOFs, the direct approach based on chiral bridging ligands is the more promising, and many improvements have still to be carried out. In this regard, the development of easily accessible chiral atropisomeric 4,4'-bipyridine ligands represents an important step toward the design of novel homochiral MOFs. Atropisomeric 4,4'-bipyridines are very rare in the literature compared to their biphenyl analogues,<sup>13</sup> and two examples have been only recently described. In 2008, Schalley et al. have reported the synthesis of 3,3'-dimethyl-5,5'-disubstituted-4,4'-bipyridines starting from 3,3',5,5'-tetramethyl-4,4'-bipyridine.<sup>14</sup> In 2012, our group widened the family of 3,3',5,5'-tetrasubstituted-4,4'-bipyridines by using a chiral tetrahalogenated 4,4'-bipyridine as the key starting material (Figure 1).<sup>15,16</sup>

Herein, we report new chiral configurationally stable 4,4'-bipyridines based on the directed deprotolithiation of tetrahalogenated achiral 4,4'-bipyridine **1** in the presence of *n*-BuLi. The enantiomers were separated by high-performance

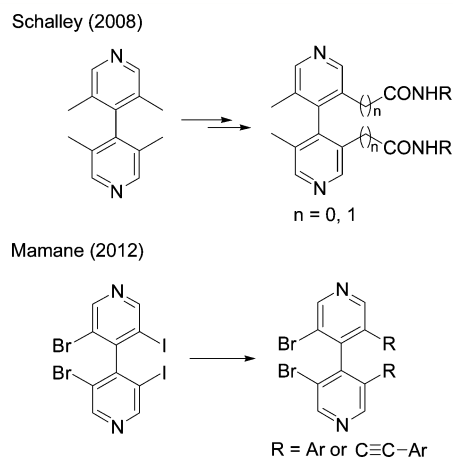


**Figure 1.** Atropisomeric 4,4'-bipyridines described in the literature.

liquid chromatography (HPLC) using immobilized polysaccharide-based chiral stationary phases, and the absolute configurations were determined by X-ray diffraction (XRD) and by correlation with the HPLC elution order of similar enantiomers of known absolute configuration.

**Received:** June 13, 2013

## RESULTS AND DISCUSSION

Recently we observed that the presence of halogen atoms of different nature offers the possibility to selectively tune the reactivity of the 4,4'-bipyridine system.<sup>15</sup> In the case of 3,3'-diodo-5,5'-dibromo-4,4'-bipyridine, the iodine acts as a regioselective modulator in cross-coupling processes under Suzuki and Sonogashira reaction conditions leading to the corresponding 3,3'-disubstituted-5,5'-dibromo-4,4'-bipyridines. The substituents surrounding the chiral axis make the chiral 4,4'-bipyridine conformationally stable, and importantly, the surviving halogen moiety is suitable for further selective transformations, thus opening the way to more complex and interesting structures. Aimed at extending the potential of the 4,4'-bipyridine system, a new molecular platform suitable for access to a new family of chiral polyhalogenated 4,4'-bipyridines starting from 2,2'-dichloro-5,5'-dibromo-4,4'-bipyridine **1** was envisaged. In this particular case, the presence of a substituent at the 2-position is worthy of special interest because it allows steric and electronic control of the nitrogen sites.

The synthetic strategy we conceived is based on the monofunctionalization at the 3-position of **1** through a metalation–electrophilic trapping sequence. It is worth noting that compound **1** containing hydrogen substituents at the 3- and 3'-positions possesses a low energy barrier to rotation around the 4,4' axis; the formation of rotational conformers (atropisomers) is thus avoided, and the 4,4' axis does not represent a chiral axis. In contrast, bulky substituents at the 3-position induce a higher energy barrier to rotation around the 4,4' axis leading to molecular chirality (Figure 2).

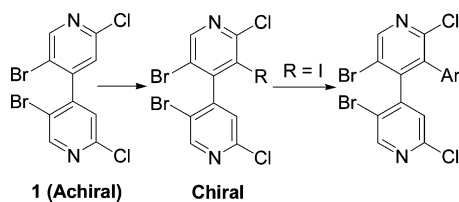
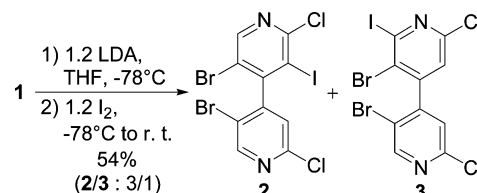


Figure 2. New family of chiral 4,4'-bipyridines.

The nature of the heteroaromatic aza-rings of **1** suggests an unpredictable reactivity arising from the presence of halogenated substituents linked at the 2,2' and 5,5' positions, which can both competitively drive the reactivity of the aromatic ring due to different mesomeric and inductive effects. Consequently, for the monofunctionalization of the 3-position, we first considered in detail the behavior of **1** toward metalation processes promoted by lithium reagents.<sup>17</sup> Taking into account that lithium diisopropylamide (LDA) is well-known to promote the directed deprotonation of halopyridines avoiding lithium–halogen exchange, the reactivity of **1** toward this reagent was explored by quenching the lithium derivative with I<sub>2</sub>, which leads to the formation of an inseparable mixture of **2** and **3** in a 3:1 ratio as the result of the competitive metalation involving positions 3 and 6 of **1** (Scheme 1).

Polyhalogenopyridines can also be deprotonated by alkyllithium compounds,<sup>14</sup> even in the presence of bromine atoms.<sup>18,19</sup> Therefore, *t*-BuLi, *s*-BuLi, and *n*-BuLi were tested at different temperatures and base concentrations in order to carry out the deprotonation of **1**. The results of these experiments were evaluated through the analysis of the crude reaction mixtures after trapping of the intermediates with I<sub>2</sub>. In all cases,

Scheme 1. Reactivity of **1** in the Presence of LDA

both the GC–MS and <sup>1</sup>H NMR analyses revealed that, along with the desired product **2**, several regioisomeric bipyridine derivatives arising from competitive reaction pathways were present in the reaction mixture (Figure 3).

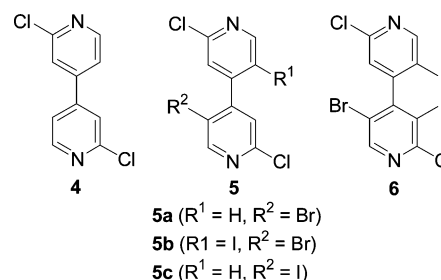


Figure 3. Other bipyridines observed during the lithiation of **1**.

Table 1 compiles the most representative results made in order to optimize the formation of **2**. Importantly, among the

Table 1. Reactivity of **1** in the Presence of Alkyllithium Bases<sup>a</sup>

entry	base ( <i>n</i> equiv), T (°C)	<b>1</b> (%)	<b>2</b> (%)	<b>4</b> (%)	<b>5</b> (%)	<b>6</b> (%)
1	<i>t</i> -BuLi (1.2), -78	25	27	31	17	0
2	<i>s</i> -BuLi (1.2), -78	63	5	20	12	0
3	<i>n</i> -BuLi (1.2), -78	6	29	12	38	15
4	<i>n</i> -BuLi (1.2), -95	15	21	12	47	5
5	<i>n</i> -BuLi (1.0), -78	15	36	11	35	3
6	<i>n</i> -BuLi (1.0), -70	3	28	20	33	16
7	<i>n</i> -BuLi (0.8), -70	29	24	17	30	0
8	<i>n</i> -BuLi (0.8), -60	10	55 (41)	25 (20)	10	0
9	<i>n</i> -BuLi (0.8), -50	0	64 (15)	28	8	0
10	<i>n</i> -BuLi (1.4), -60	0	0	33 (22)	9	58 (36)
11	<i>n</i> -BuLi (1.6), -60	0	0	26	10	37 <sup>b</sup>
12	-78, slow addition	6	48 (28)	46	0	0
13	PhLi (0.8), -78, slow addition	15	56 (40)	22	7	

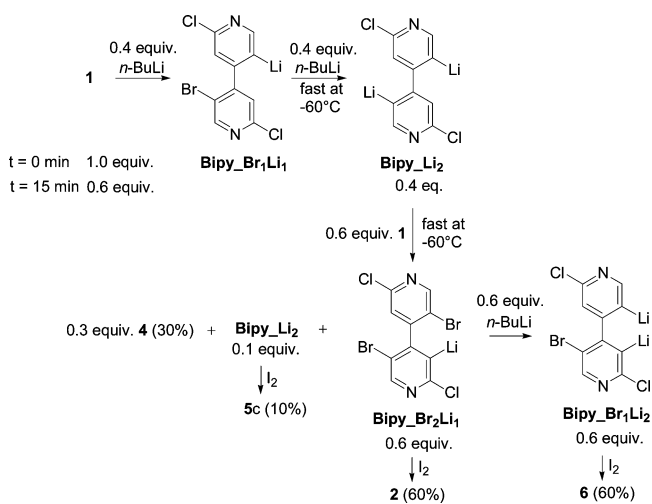
<sup>a</sup>THF was used as the solvent in all experiments. <sup>b</sup>27% of nonidentified products.

secondary compounds shown in Figure 3, we were delighted to observe the formation of dissymmetric 5-bromo-2,2'-dichloro-3,5'-diiodo-4,4'-bipyridine **6** deciding also to improve its formation. Starting from **1**, compounds **4**<sup>7</sup> and **5a–c** arise from bromine–lithium exchanges, whereas bipyridine **6** is the result of both a lithiation and bromine–lithium exchange. Such dual reactivity of organolithium compounds in the same pot was already observed with 2,4,6-triphenylbromobenzene<sup>20</sup> and 4,4'-dibromo-3,3'-bithiophene.<sup>21</sup>

Among the three alkyllithium bases which were compared under the same reaction conditions ( $-78\text{ }^{\circ}\text{C}$ , 1.2 equiv of alkyllithium, entries 1–3, Table 1), *n*-BuLi gave the best conversion (entry 3). Although the formation of **2** was comparable by using *t*-BuLi and *n*-BuLi (compare entries 1 and 3), the latter was chosen for a further optimization study and, in addition, in order to evaluate the formation of bipyridine **6** which was exclusively observed carrying out the reaction in the presence of this base (entry 3, Table 1). This product can be almost completely avoided by decreasing the temperature (entry 4) or by using only 1 equiv of *n*-BuLi (entry 5). The conversion was, however, lower in these two last cases. More importantly, decreasing the temperature caused an increase of the bromine–lithium exchange products **5** (entry 4). Increasing the temperature to  $-70\text{ }^{\circ}\text{C}$  has the reverse effect, but the formation of **6** became high (entry 6). Decreasing again the amount of *n*-BuLi to 0.8 equiv allowed the complete disappearance of **6** but with lower conversion (entry 7). Finally, it was found that 0.8 equiv of *n*-BuLi at  $-60\text{ }^{\circ}\text{C}$  were the best conditions to achieve a good conversion with no formation of **6** (entry 8). In this case, bipyridine **2** could be isolated with 41% yield. Increasing the temperature to  $-50\text{ }^{\circ}\text{C}$  caused degradation as shown by the lower yield of 15% (entry 9). It is worth noting that under conditions of entry 8, the amount of **4** was the same independently of the quantity of  $\text{I}_2$  added at the end of the reaction. It is probable that this compound is formed during the lithiation step (vide infra). Bipyridine **6** could be obtained selectively by increasing the amount of *n*-BuLi. The best result was obtained with 1.4 equiv of *n*-BuLi (entry 10) and higher amount resulted in the formation of other secondary products (entry 11). Under conditions of entry 10, the chiral bipyridine **6** was isolated with 36% yield and the amount of **2** was almost unchanged compared to entry 8. The reaction could be performed at  $-78\text{ }^{\circ}\text{C}$  by slow addition (30 min) of 0.8 equiv of *n*-BuLi, but the amount of compound **4** increased (entry 12). Substitution of *n*-BuLi by PhLi could maintain the formation of **4** at a low level (entry 13), and the yield of **2** was comparable to entry 8.

On the basis of our observations, a rationalization can be proposed as follows (Scheme 2). Bipyridine **1** reacts rapidly with *n*-BuLi in bromine–metal exchange reiterated process to produce **Bipy** $\text{-Br}_1\text{Li}_1$  and, in turn, **Bipy** $\text{-Li}_2$ . The second

### Scheme 2. Proposed Mechanism for the Formation of **2** and **6**



bromine–lithium exchange is faster at  $-60\text{ }^{\circ}\text{C}$  probably because the steric hindrance around the C4 – C4' bond is higher in **1** than in **Bipy** $\text{-Br}_1\text{Li}_1$ . Moreover, the influence of the negative charge for the second bromine–lithium exchange is negligible due to the independent nature of the two pyridine parts. **Bipy** $\text{-Li}_2$  (0.3 equiv) can then react with the remaining amount of **1** to give **Bipy** $\text{-Br}_2\text{Li}$  and **4** in a 2:1 ratio.<sup>22</sup> This deprotonation step is slow below  $-78\text{ }^{\circ}\text{C}$  while it is fast above  $-60\text{ }^{\circ}\text{C}$ . During the final step of the reaction, **Bipy** $\text{-Br}_2\text{Li}$  as well as unreacted **Bipy** $\text{-Li}_2$  (0.1 equiv) can react with  $\text{I}_2$  furnishing **2** and **5c**, respectively. When 1.4 equiv of *n*-BuLi is used, the excess (0.6 equiv) can react with **Bipy** $\text{-Br}_2\text{Li}$  to give **Bipy** $\text{-BrLi}_2$ , which, after quenching with  $\text{I}_2$ , generates **6**. This result indicates that the sequence **1** to **Bipy** $\text{-Br}_2\text{Li}$  through **Bipy** $\text{-Li}_2$  is very fast. According to this mechanism, **2** and **6** cannot exceed 60% in yield. During the slow addition of *n*-BuLi at  $-78\text{ }^{\circ}\text{C}$  (entry 12), the higher amount of **4** can be explained taking into account the reaction between **Bipy** $\text{-Li}_2$  and *n*-BuBr (formed by lithium–bromine exchange from **1** and *n*-BuLi) with concomitant formation of butene and LiBr. This reaction is not allowed with PhBr formed after lithium–bromine exchange between **Bipy** $\text{-Li}_2$  and PhLi (entry 13); therefore, the amount of **4** remains unchanged compared to entry 8.

Under the best reaction conditions (0.8 equiv of *n*-BuLi,  $-60\text{ }^{\circ}\text{C}$ ) previously established, a family of chiral compounds was obtained by the deprotonation of **1**. It was observed that different electrophiles reacted smoothly thus providing the way to the direct access to racemic 3-substituted 5,5'-dibromo-2,2'-dichloro-4,4'-bipyridines **7** (Table 2). Chiral 4,4'-bipyridines **7**

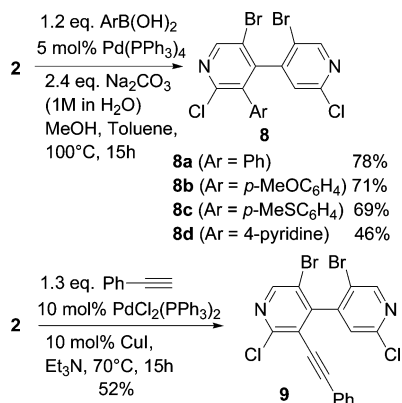
Table 2. Electrophile Scope after Deprotonation of **1**

electrophile	product	yield (%)
MeI	<b>7a</b> (R = Me)	46
MeSSMe	<b>7b</b> (R = SMe)	32
ClSiMe <sub>3</sub>	<b>7c</b> (R = SiMe <sub>3</sub> )	53
ClSnMe <sub>3</sub>	<b>7d</b> (R = SnMe <sub>3</sub> )	33
ClSnBu <sub>3</sub>	<b>7e</b> (R = SnBu <sub>3</sub> )	45
ClPPh <sub>2</sub>	<b>7f</b> (R = POPh <sub>2</sub> ) <sup>a</sup>	46

<sup>a</sup>The product was oxidized during the purification on silica gel.

bearing alkyl, sulfur, silyl, stannyl, and phosphine functional groups were isolated in the reported yields. In this context, it is important to remember that due to the particular reaction pathway here operative, the process cannot exceed 60% in the overall yield. In the case of **7f**, the phosphine group underwent spontaneous oxidation during the chromatographic treatment on silica gel. In all cases, bipyridine **4** was formed with approximately 20% yield.

Having at disposal chiral compound **2**, a different family of chiral 4,4'-bipyridines derivatives was obtained by cross-coupling **2** with a series of boronic acids and phenylacetylene (Scheme 3). The Suzuki reaction was performed under standard conditions with 1.2 equiv of either phenyl-, 4-methoxyphenyl-, 4-(methylthio)phenyl-, or 4-pyridylboronic acid to give the desired bipyridines **8** in 46 to 78% yields

Scheme 3. Cross-Coupling Reactions of **2**

(Scheme 3). Concerning the Sonogashira coupling, the overcoupling products have been limited by using 1.3 equiv of phenylacetylene, thus giving bipyridine **9** in a 52% yield.

All the atropisomeric 3-substituted 5,5'-dibromo-2,2'-dichloro-4,4'-bipyridines<sup>23</sup> as well as bipyridine **6** were enantioseparated by HPLC on immobilized polysaccharide-based chiral stationary phases, namely Chiralpak IA and Chiralpak IC, which exhibited complementary enantioseparation properties (Table 3). For instance, 500 mg of racemic bipyridine **2** was separated on Chiralpak IA, furnishing pure enantiomers (>99% ee).<sup>24</sup>

**Table 3. Absolute Configurations of All 4,4'-Bipyridine Atropisomers**

bipyridine	HPLC column	absolute configuration <sup>a</sup> (ee, %)	
		1st eluted peak	2nd eluted peak
<b>2</b>	Chiralpak IA	<i>P</i> (>99)	<i>M</i> (>99)
<b>6</b>	Chiralpak IA	<i>P</i> (>99)	<i>M</i> (>99)
<b>7a</b>	Chiralpak IC	<i>M</i> (>99)	<i>M</i> (>99)
<b>7b</b>	Chiralpak IC	<i>M</i> (>99)	<i>M</i> (>99)
<b>7c</b>	Chiralpak IC	<i>M</i> (>99)	<i>P</i> (>99)
<b>7d</b>	Chiralpak IC	<i>P</i> (>99)	<i>M</i> (>99)
<b>7f</b>	Chiralpak IA	<i>M</i> (>99)	<i>P</i> (99)
<b>8a</b>	Chiralpak IC	<i>M</i> (>99)	<i>P</i> (>99)
<b>8b</b>	Chiralpak IC	<i>M</i> (>99)	<i>P</i> (>99)
<b>8c</b>	Chiralpak IC	<i>M</i> (>99)	<i>P</i> (>99)
<b>8d</b>	Chiralpak IA	<i>M</i> (>99)	<i>P</i> (>99)
<b>9</b>	Chiralpak IA	<i>M</i> (>99)	<i>P</i> (99)

<sup>a</sup>The assignment of the reported absolute configurations were achieved by XRD for **2**, **6**, **7c,d**, **8a**, and **9** and by correlation from HPLC data for **7a,b,f** and **8b,c**.

Compared to 3,3',5,5'-tetrasubstituted-4,4'-bipyridines,<sup>15</sup> the new 4,4'-bipyridines showed much lower signals in electronic circular dichroism (ECD) rendering the absolute configuration determination very problematic by this method (coupled with time-dependent density functional theory calculations). However, in several cases, single crystals were obtained and the absolute configuration could be assigned by single-crystal XRD with the help of anomalous dispersion (Table 3 and Supporting Information).<sup>25</sup> For 4,4'-bipyridines **2** and **6**, in addition to the absolute configuration determination, XRD was helpful in order to unambiguously assign their structure (Figures S1 and S2 in Supporting Information). Due to the presence of a high number of halogen atoms substituent on the bipyridyl rings, the

crystal packing of these two compounds is characterized by numbers of halogen...Lewis base and halogen...halogen interactions. For example, in **2** a cyclic I,Br...N motif binds the two crystallographic independent molecules (Br1...N19 = 3.083 Å; C5—Br1...N19 = 175.9°; I2...N7 = 3.070 Å; C15—I2...N7 = 176.0°) with the  $\sigma$ -hole of the halogen atoms pointing toward the nitrogen atoms of a neighboring molecule (Figure 4).

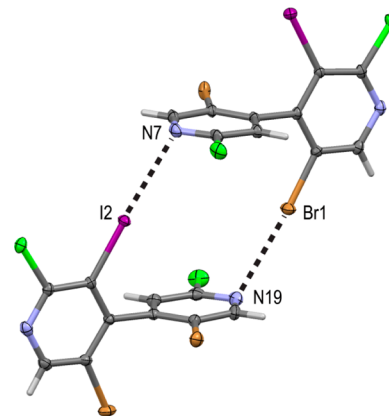
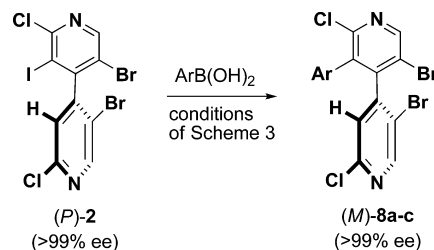


**Figure 4.** ORTEP plots of the asymmetric unit of **2**, showing the cyclic halogen (I2, Br1)...Lewis base (N7, N19) intermolecular interaction. Atomic displacement parameter ellipsoids set at 50% probability and hydrogen atoms shown as sticks.

The absolute configuration determination for compounds **7a,b,f** and **8b,c** was not achievable by XRD because these compounds could not be crystallized. For compounds **8b,c**, the absolute configuration was deduced from the results of the Suzuki reaction between 4,4'-bipyridine (*P*)-**2** and phenyl, 4-methoxyphenyl, and 4-(methylthio)phenyl boronic acids. Indeed, (*P*)-**2** reacted with phenylboronic acid to give (*M*)-**8a** demonstrating that the Suzuki coupling is completely stereospecific, as observed previously in the case of 3,3'-dibromo-5,5'-diiodo-4,4'-bipyridine.<sup>15</sup> Therefore, under the same conditions, we assume that (*P*)-**2** gave (*M*)-**8b** and (*M*)-**8c** (Scheme 4).

**Scheme 4. Stereoconservative Coupling of (*P*)-**2****



Finally, for compounds **7a,b,f**, the absolute configuration was determined by correlation with the HPLC elution order of the similar compounds **2**, **6**, **7c,d**, **8a,d**, and **9** of known absolute configuration (see discussion in the Supporting Information).

■ **CONCLUSION**

We have developed an efficient way to prepare chiral polyhalogenated 4,4'-bipyridines through a directed deprotonation reaction of a symmetrical prochiral 4,4'-bipyridine and subsequent reaction with a large set of electrophiles.

Unexpectedly, *n*-BuLi can drive either the deprotonation process alone or the simultaneous deprotonation and bromine–lithium exchange. However, a deep analysis of product distribution has revealed that *n*-BuLi was not directly involved in the deprotonation process. Probably *n*-BuLi first performs bromine–lithium exchange reactions with **1** to generate a dilithiated species which is proposed to be the key intermediate in the deprotonation reaction. Once the first lithiated species is formed, further bromine–lithium exchange can occur. After trapping with iodine, the mono- and dilithiated species give access to chiral pentahalogenated 4,4'-bipyridines which represent valuable intermediates for the preparation of functionalized chiral derivatives through cross-coupling reactions. For instance, bipyridine **2** bearing only one iodine atom was successfully functionalized through Suzuki and Sonogashira couplings. All the reported 4,4'-bipyridines could be enantioselectively separated by HPLC and the absolute configurations of the obtained enantiomers were assigned by means of XRD and comparative HPLC elution. The asymmetric versions of the reported lithiation reactions and the reactivity of bipyridine **6** are under investigation and will be reported in due course.

## EXPERIMENTAL SECTION

**General Experimental Methods.** All reactions were performed under an atmosphere of argon in oven-dried glassware. Tetrahydrofuran (THF) was distilled over sodium/benzophenone and stored over sodium. All other solvents and reagents were used as received. TLC was performed on silica gel plates and visualized with a UV lamp (254 nm). Chromatography was performed on silica gel (70–230 mesh). All melting points were uncorrected. The <sup>1</sup>H and <sup>13</sup>C NMR spectra were recorded at 200 and 50 MHz, respectively. Chemical shifts are quoted in parts per million (ppm) downfield of tetramethylsilane. Coupling constants *J* are quoted in hertz. Mass spectra were recorded using EI at 70 eV and high resolution mass spectra were recorded using APCL.

For chiral HPLC analyses, a high-pressure binary gradient system equipped with a diode-array detector operating at 254 (220, 280) nm and a 20 μL sample loop was employed. Chiralpak IA (amylose tris-3,5-dimethylphenylcarbamate) and Chiralpak IC (cellulose tris-3,5-dichlorophenylcarbamate) (250 × 4.6 mm) (5 μm) were used as chiral columns. HPLC-grade solvents were purchased and used as received. Analyses were performed in isocratic mode. Normal phase was used as elution mode, at 22 °C.

Crystal structures of bipyridines **2** (first eluted peak), **6** (first eluted peak), **7c** (first eluted peak), **7d** (second eluted peak), **8a** (first eluted peak), **8d** (first eluted peak), and **9** (first eluted peak) were determined by single-crystal X-ray diffraction using either Mo or Cu Kα radiations (Supernova Dual source diffractometer, Agilent Technologies) at low temperature (*T* = 110 K).

**Lithiation Procedure of 1 with 0.8 equiv of *n*-BuLi (Table 1, entry 8): Formation of 2 and 4.** Bipyridine **1** (1.38 mmol, 530 mg) in THF (5.5 mL) was cooled to –60 °C. *n*-BuLi (1.3 M in hexanes, 1.1 mmol, 0.85 mL) was added dropwise, and the mixture was stirred at –60 °C for 15 min. After the mixture was cooled to –78 °C, I<sub>2</sub> (1.38 mmol, 351 mg) in THF (1.4 mL) was added dropwise and the temperature was raised to ambient. A saturated aqueous solution of Na<sub>2</sub>S<sub>2</sub>O<sub>3</sub> (1 mL) was added, and the mixture was extracted with dichloromethane (2 × 25 mL). The organic phases were combined, washed with brine, and dried over MgSO<sub>4</sub>. After concentration, the mixture was purified by chromatography on silica gel (eluent: cyclohexane/ethyl acetate 95/5) to give **2** as a white solid (290 mg, 41%). Increasing gradually the eluent ratio to 1/1 furnished **4** as a white solid (62 mg, 20%).

**5,5'-Dibromo-2,2'-dichloro-3-iodo-4,4'-bipyridinyl (2):** mp 164–166 °C; <sup>1</sup>H NMR (CDCl<sub>3</sub>, 200 MHz) δ = 7.11 (s, 1H), 8.57 (s, 1H), 8.68 (s, 1H) ppm; <sup>13</sup>C NMR (CDCl<sub>3</sub>, 50 MHz) δ = 99.5, 117.5, 118.5, 124.3, 150.5, 152.4, 153.1, 155.0 ppm; MS (ESI) *m/z*

507 (M, 25), 429 (M – Br, 100), 381 (M – I, 23), 302 (M – Br – I, 30); HRMS calcd for C<sub>10</sub>H<sub>4</sub>Br<sub>2</sub>Cl<sub>2</sub>I<sub>2</sub>N<sub>2</sub> (M + H) 506.7157, found 506.7159.

**2,2'-Dichloro-4,4'-bipyridinyl (4):** mp 238–240 °C; <sup>1</sup>H NMR (CDCl<sub>3</sub>, 200 MHz) δ = 7.43 (dd, *J* = 5.2, 1.4 Hz, 2H), 7.56 (d, *J* = 1.4 Hz, 2H), 8.54 (d, *J* = 5.2 Hz, 2H) ppm; <sup>13</sup>C NMR (CDCl<sub>3</sub>, 50 MHz) δ = 120.2, 122.1, 147.4, 150.7, 152.8 ppm; MS (ESI) *m/z* 224 (M, 100%), 189 (M – Cl, 65), 153 (M – Cl<sub>2</sub>, 50), 302.

**Lithiation Procedure of 1 with 0.8 equiv of PhLi (Table 1, Entry 13).** Bipyridine **1** (1 mmol, 383 mg) in THF (4 mL) was cooled to –78 °C. PhLi (1.8 M in *n*-Bu<sub>2</sub>O, 0.8 mmol, 0.45 mL) was added slowly during 30 min, and the mixture was stirred at –78 °C for 30 min. After the mixture was cooled to –78 °C, I<sub>2</sub> (1 mmol, 254 mg) in THF (1 mL) was added dropwise, and the temperature was raised to ambient. A saturated aqueous solution of Na<sub>2</sub>S<sub>2</sub>O<sub>3</sub> (1 mL) was added, and the mixture was extracted with dichloromethane (2 × 20 mL). The organic phases were combined, washed with brine, and dried over MgSO<sub>4</sub>. After concentration, the mixture was purified by chromatography on silica gel (eluent: cyclohexane/ethyl acetate 95/5) to give **2** as a white solid (204 mg, 40%).

**Lithiation Procedure of 1 with 1.4 equiv of *n*-BuLi (Table 1, Entry 10): Formation of 6.** Bipyridine **1** (0.5 mmol, 192.5 mg) in THF (2 mL) was cooled to –60 °C. *n*-BuLi (1.3 M in hexanes, 0.7 mmol, 0.54 mL) was added dropwise during 10 min, and the mixture was stirred at –60 °C for 15 min. After being cooled to –78 °C, I<sub>2</sub> (1 mmol, 254 mg) in THF (1 mL) was added dropwise, and the temperature was raised to ambient. A saturated aqueous solution of Na<sub>2</sub>S<sub>2</sub>O<sub>3</sub> (1 mL) was added and the mixture was extracted with dichloromethane (2 × 15 mL). The organic phases were combined, washed with brine and dried over MgSO<sub>4</sub>. After concentration, the mixture was purified by chromatography on silica gel (eluent: cyclohexane/ethyl acetate 95/5) to give **6** as a white solid (100 mg, 36%).

**5-Bromo-2,2'-dichloro-3,5'-iodo-4,4'-bipyridinyl (6):** mp 162–164 °C; <sup>1</sup>H NMR (CDCl<sub>3</sub>, 200 MHz) δ = 7.10 (d, *J* = 0.4 Hz, 1H), 8.57 (s, 1H), 8.87 (d, *J* = 0.4 Hz, 1H) ppm; <sup>13</sup>C NMR (CDCl<sub>3</sub>, 50 MHz) δ = 93.8, 99.7, 117.6, 124.1, 150.6, 152.1, 155.2, 155.3, 156.5, 157.8 ppm; MS (ESI) *m/z* 555 (M, 30), 429 (M – I, 100), 348 (M – Br – I, 10), 302 (M – I<sub>2</sub>, 15); HRMS calcd for C<sub>10</sub>H<sub>4</sub>BrCl<sub>2</sub>I<sub>2</sub>N<sub>2</sub> (M + H) 554.7019, found 554.7042.

**Typical Procedure for the Preparation of 7.** Bipyridine **1** (0.5 mmol, 192.5 mg) in THF (2 mL) was cooled to –60 °C. *n*-BuLi (1.3 M in hexanes, 0.4 mmol, 0.3 mL) was added dropwise, and the mixture was stirred at –60 °C for 15 min. After being cooled to –78 °C, electrophile (1 mmol) in THF (0.5 mL) was added dropwise and the temperature was raised to ambient. Water (1 mL) was added and the mixture was extracted with dichloromethane (2 × 15 mL). The organic phases were combined, washed with brine, and dried over MgSO<sub>4</sub>. After concentration, the mixture was purified by chromatography on silica gel (eluent: cyclohexane/ethyl acetate 9/1 except for **7f**: 3/1) to give **7**.

**5,5'-Dibromo-2,2'-dichloro-3-methyl-4,4'-bipyridinyl (7a):** mp 76–78 °C; <sup>1</sup>H NMR (CDCl<sub>3</sub>, 200 MHz) δ = 2.15 (s, 3H), 7.14 (s, 1H), 8.51 (s, 1H), 8.68 (s, 1H) ppm; <sup>13</sup>C NMR (CDCl<sub>3</sub>, 50 MHz) δ = 17.9, 119.0, 119.1, 124.6, 132.0, 147.2, 148.7, 149.1, 151.0, 151.3, 152.3 ppm; MS (ESI) *m/z* 396 (M, 100), 317 (M – Br, 35), 279 (M – Br – Cl, 16), 236 (M – Br<sub>2</sub>, 20), 200 (M – Br<sub>2</sub> – Cl, 30); HRMS calcd for C<sub>11</sub>H<sub>7</sub>Br<sub>2</sub>Cl<sub>2</sub>N<sub>2</sub> (M + H) 394.8348, found 394.8356.

**5,5'-Dibromo-2,2'-dichloro-3-(methylthio)-4,4'-bipyridinyl (7b):** mp 88–90 °C; <sup>1</sup>H NMR (CDCl<sub>3</sub>, 200 MHz) δ = 2.38 (s, 3H), 7.11 (s, 1H), 8.59 (s, 1H), 8.66 (s, 1H) ppm; <sup>13</sup>C NMR (CDCl<sub>3</sub>, 50 MHz) δ = 18.4, 118.9, 119.0, 124.5, 133.0, 149.7, 150.6, 150.65, 151.9, 152.3, 155.6 ppm; MS (ESI) *m/z* 349 (M – Br, 100), 334 (M – Br – CH<sub>3</sub>, 65); HRMS calcd for C<sub>11</sub>H<sub>7</sub>Br<sub>2</sub>Cl<sub>2</sub>N<sub>2</sub>S (M + H) 426.8068, found 426.8056.

**5,5'-Dibromo-2,2'-dichloro-3-trimethylsilyl-4,4'-bipyridinyl (7c):** mp 116–118 °C; <sup>1</sup>H NMR (CDCl<sub>3</sub>, 200 MHz) δ = 0.12 (s, 9H), 7.12 (s, 1H), 8.58 (s, 1H), 8.60 (s, 1H) ppm; <sup>13</sup>C NMR (CDCl<sub>3</sub>, 50 MHz) δ = 0.8, 120.35, 120.4, 125.3, 135.1, 150.4, 150.8, 151.6, 151.7, 153.2, 156.7 ppm; MS (ESI) *m/z* 439 (M – CH<sub>3</sub>, 75), 403 (M – Cl –

CH<sub>3</sub>, 55), 73 (Si(CH<sub>3</sub>)<sub>3</sub>, 100); HRMS calcd for C<sub>13</sub>H<sub>13</sub>Br<sub>2</sub>Cl<sub>2</sub>N<sub>2</sub>Si (M + H) 452.8586, found 452.8618.

**5,5'-Dibromo-2,2'-dichloro-3-(trimethylstannanyl)-4,4'-bipyridinyl (7d):** mp 100–102 °C; <sup>1</sup>H NMR (CDCl<sub>3</sub>, 200 MHz) δ = 0.11 (m, J(<sup>1</sup>H–<sup>119</sup>Sn) = 56.8 Hz, J(<sup>1</sup>H–<sup>117</sup>Sn) = 54.8 Hz, 9H), 7.13 (s, 1H), 8.52 (s, 1H), 8.62 (s, 1H) ppm; <sup>13</sup>C NMR (CDCl<sub>3</sub>, 50 MHz) δ = –6.1, 119.8, 120.0, 125.2, 140.1, 150.65, 150.7, 151.6, 152.0, 155.0, 157.8 ppm; MS (ESI) *m/z* 529 (M – CH<sub>3</sub>, 100), 164 (Sn(CH<sub>3</sub>)<sub>3</sub>, 20), 155 (50); HRMS calcd for C<sub>13</sub>H<sub>13</sub>Br<sub>2</sub>Cl<sub>2</sub>N<sub>2</sub>Sn (M + H) 544.7814, found 544, 7801.

**5,5'-Dibromo-2,2'-dichloro-3-(tributylstannanyl)-4,4'-bipyridinyl (7e):** <sup>1</sup>H NMR (CDCl<sub>3</sub>, 200 MHz) δ = 0.70–0.90 (m, 15H), 1.10–1.50 (m, 12H), 7.06 (s, 1H), 8.50 (s, 1H), 8.61 (s, 1H) ppm; <sup>13</sup>C NMR (CDCl<sub>3</sub>, 50 MHz) δ = 12.0, 13.5, 27.0, 28.7, 119.8, 120.1, 125.2, 140.9, 150.7, 151.1, 151.3, 151.8, 155.4, 158.0 ppm; MS (ESI) *m/z* 615 (M – C<sub>4</sub>H<sub>9</sub>, 35), 429 (M – (C<sub>4</sub>H<sub>9</sub>)<sub>2</sub>, 25), 57 (C<sub>4</sub>H<sub>9</sub>, 100); HRMS calcd for C<sub>22</sub>H<sub>31</sub>Br<sub>2</sub>Cl<sub>2</sub>I<sub>2</sub>N<sub>2</sub>Sn (M + H) 670.9224, found 670.9251.

**5,5'-Dibromo-2,2'-dichloro-3-(diphenylphosphinoyl)-4,4'-bipyridinyl (7f):** mp 105–107 °C; <sup>1</sup>H NMR (CDCl<sub>3</sub>, 200 MHz) δ = 6.89 (s, 1H), 7.40–7.80 (m, 10H), 8.44 (s, 1H), 8.80 (d, J(<sup>1</sup>H–<sup>31</sup>P) = 1.6 Hz, 1H) ppm; <sup>13</sup>C NMR (CDCl<sub>3</sub>, 50 MHz) δ = 119.8, 122.4 (J = 6.5 Hz), 124.3, 128.6 (J = 13.2 Hz), 128.8 (J = 12.8), 129.8, 129.8, 131.0 (J = 80.4 Hz), 131.7 (8.0 Hz), 131.9 (J = 8.4 Hz), 132.5 (J = 2.9 Hz), 132.7 (J = 2.9 Hz), 149.1 (J = 2.9 Hz), 149.8, 151.0, 152.7 (J = 6.4 Hz), 152.7 (J = 6.4 Hz), 153.5 (J = 6.2 Hz), 154.2 (J = 1 Hz) ppm. <sup>31</sup>P NMR (CDCl<sub>3</sub>, 121 MHz) δ = 26.9 ppm; MS (ESI) *m/z* 503 (M – Br, 85), 387 (M – Br<sub>2</sub> – Cl, 30), 77 (C<sub>6</sub>H<sub>5</sub>, 100); HRMS calcd for C<sub>22</sub>H<sub>13</sub>Br<sub>2</sub>Cl<sub>2</sub>N<sub>2</sub>OP (M + H) 580.8583, found 580.8576.

**Typical Procedure for the Preparation of 8a–c.** To a degassed toluene solution (1 mL) containing Pd(PPh<sub>3</sub>)<sub>4</sub> (5.8 mg, 0.01 mmol) and bipyridine 2 (50.9 mg, 0.1 mmol) were successively added degassed solutions of arylboronic acid (0.12 mmol, 1.2 equiv) in methanol (0.5 mL) and Na<sub>2</sub>CO<sub>3</sub> (25.5 mg, 0.24 mmol) in water (0.5 mL). After heating for 12h at 100 °C, the reaction mixture was cooled to room temperature, extracted with ethyl acetate, and dried over MgSO<sub>4</sub>. After concentration, the residue was purified by chromatography on silica gel to give bipyridine 8a–c.

**5,5'-Dibromo-2,2'-dichloro-3-phenyl-4,4'-bipyridinyl (8a):** mp 225–227 °C; <sup>1</sup>H NMR (CDCl<sub>3</sub>, 200 MHz) δ = 6.94 (s, 1H), 7.05–7.40 (m, 6H), 8.43 (s, 1H), 8.67 (s, 1H) ppm; <sup>13</sup>C NMR (CDCl<sub>3</sub>, 50 MHz) δ = 119.4, 119.5, 125.2, 128.25, 128.3, 128.6, 129.0, 129.2, 134.4, 137.0, 147.4, 148.8, 150.1, 150.4, 150.5, 151.7 ppm; MS (ESI) *m/z* 458 (M, 25), 429 (M – Br – Cl, 70), 262 (M – Br<sub>2</sub> – Cl, 100), 227 (M – Br<sub>2</sub> – Cl<sub>2</sub>, 40); HRMS calcd for C<sub>16</sub>H<sub>9</sub>Br<sub>2</sub>Cl<sub>2</sub>N<sub>2</sub> (M + H) 456.8504, found 456.8495.

**5,5'-Dibromo-2,2'-dichloro-3-(4-methoxyphenyl)-4,4'-bipyridinyl (8b):** <sup>1</sup>H NMR (CDCl<sub>3</sub>, 200 MHz) δ = 3.78 (s, 3H), 6.80 (t, J = 9.4 Hz, 2H), 6.95 (s, 1H), 7.02 (d, J = 8.3 Hz, 1H), 7.08 (d, J = 8.3 Hz, 1H), 8.44 (s, 1H), 8.64 (s, 1H) ppm; <sup>13</sup>C NMR (CDCl<sub>3</sub>, 50 MHz) δ = 55.2, 113.8, 113.9, 119.3, 125.2, 126.5, 129.7, 130.6, 136.8, 147.6, 149.0, 150.1, 151.0, 151.7, 159.7 ppm; MS (ESI) *m/z* 488 (M, 30), 409 (M – Br, 25), 373 (M – Br – Cl, 35), 292 (M – Br<sub>2</sub> – Cl, 100); HRMS calcd for C<sub>17</sub>H<sub>11</sub>Br<sub>2</sub>Cl<sub>2</sub>N<sub>2</sub>O (M + H) 486.8610, found 486.8598.

**5,5'-Dibromo-2,2'-dichloro-3-(4-(methylthio)phenyl)-4,4'-bipyridinyl (8c):** <sup>1</sup>H NMR (CDCl<sub>3</sub>, 200 MHz) δ = 2.46 (s, 3H), 6.96 (s, 1H), 7.99 (d, J = 8.2 Hz, 1H), 7.12 (s, 2H), 7.16 (d, J = 8.2 Hz, 1H), 8.45 (s, 1H), 8.66 (s, 1H) ppm; <sup>13</sup>C NMR (CDCl<sub>3</sub>, 50 MHz) δ = 15.0, 119.4, 119.45, 125.2, 125.5, 125.7, 128.8, 129.6, 130.6, 136.5, 140.3, 147.4, 148.8, 150.2, 150.4, 150.7, 151.8 ppm; MS (ESI) *m/z* 506 (M, 100), 471 (M – Cl, 60), 425 (M – Br, 15), 302 (M – Br – SCH<sub>3</sub>, 60); HRMS calcd for C<sub>17</sub>H<sub>11</sub>Br<sub>2</sub>Cl<sub>2</sub>N<sub>2</sub>S (M + H) 502.8381, found 502.8379.

**5,5'-Dibromo-2,2'-dichloro-3-(4-pyridyl)-4,4'-bipyridinyl (8d).** Bipyridine 2 (120 mg, 0.2 mmol), 4-pyridineboronic acid (85% purity, 35 mg, 0.24 mmol), and Pd(PPh<sub>3</sub>)<sub>4</sub> (11.6 mg, 0.01 mmol) were placed under argon. Dioxane (1.4 mL) was added, and the mixture was stirred for 10 min. An aqueous solution of Na<sub>2</sub>CO<sub>3</sub> (1M, 0.6 mL) was added, and the mixture was heated under reflux for 18 h. After being

cooled to room temperature, the mixture was extracted with ethyl acetate and dried over MgSO<sub>4</sub>. After concentration, the residue was purified by chromatography on silica gel (cyclohexane/ethyl acetate 3/1) to give bipyridine 8d (42 mg, 46%): mp 218–220 °C; <sup>1</sup>H NMR (CDCl<sub>3</sub>, 200 MHz) δ = 6.98 (s, 1H), 7.18 (m, 2H), 8.47 (s, 1H), 8.62 (broad s, 2H), 8.74 (s, 1H) ppm; <sup>13</sup>C NMR (CDCl<sub>3</sub>, 50 MHz) δ = 119.0, 119.7, 123.6, 124.5, 124.8, 133.6, 143.7, 146.8, 147.7, 148.8, 149.1, 149.3, 150.5, 151.6, 152.0 ppm; MS (ESI) *m/z* 459 (M, 15), 380 (M – Br, 100), 344 (M – Br – Cl, 25), 302 (M – Br<sub>2</sub> – Cl, 45); HRMS calcd for C<sub>15</sub>H<sub>8</sub>Br<sub>2</sub>Cl<sub>2</sub>N<sub>3</sub> (M + H) 475.8457, found 457.8480.

**5,5'-Dibromo-2,2'-dichloro-3-phenylethynyl-4,4'-bipyridinyl (9).** An oven-dried resealable 10-mL tube equipped with a magnetic stir bar was charged with PdCl<sub>2</sub>(PPh<sub>3</sub>)<sub>2</sub> (7 mg, 0.01 mmol), CuI (1.9 mg, 0.01 mmol), and bipyridine 2 (50.9 mg, 0.1 mmol). The tube was capped, evacuated, and backfilled with argon (with a needle). A degassed solution of phenylacetylene (13.3 mg, 0.13 mmol) in dry triethylamine (1 mL) was added, and the mixture was heated at 70 °C for 12h. The reaction mixture was then allowed to cool to room temperature, extracted with ethyl acetate, and concentrated. Purification by column chromatography on silica gel (cyclohexane/ethyl acetate 9/1) gave bipyridine 9 (25 mg, 52%): mp 119–121 °C; <sup>1</sup>H NMR (CDCl<sub>3</sub>, 200 MHz) δ = 7.16–7.24 (m, 2H), 7.28–7.39 (m, 4H), 8.58 (s, 1H), 8.71 (s, 1H) ppm; <sup>13</sup>C NMR (CDCl<sub>3</sub>, 50 MHz) δ = 81.9, 102.7, 118.3, 119.1, 121.0, 121.1, 125.0, 128.6, 129.9, 131.7, 148.6, 149.0, 150.5, 151.5, 152.1 ppm; MS (ESI) *m/z* 483 (M, 15%), 402 (M – Br, 100), 368 (M – Br – Cl, 20), 322 (M – Br<sub>2</sub> – Cl, 30), 286 (M – Br<sub>2</sub> – Cl<sub>2</sub>, 75), 252 (60), 225 (50), 99 (50); HRMS calcd for C<sub>18</sub>H<sub>9</sub>Br<sub>2</sub>Cl<sub>2</sub>N<sub>2</sub> (M + H) 480.8504, found 480.8487.

**Crystal data for 2:** C<sub>10</sub>H<sub>3</sub>Br<sub>2</sub>Cl<sub>2</sub>I<sub>2</sub>N<sub>2</sub>, *M* = 508.74, triclinic, *a* = 6.8899(1) Å, *b* = 9.0638(1) Å, *c* = 11.7741(2) Å, α = 90.773(1)°, β = 101.424(1)°, γ = 111.340(1)°, *V* = 668.341(17) Å<sup>3</sup>, *T* = 110(2) K, space group *P*1, *Z* = 2, μ(Mo *K*α) = 8.750 mm<sup>–1</sup>, 65157 reflections measured, 13261 independent reflections (*R*<sub>int</sub> = 0.0311). Flack parameter = 0.001(3). The final *R*<sub>1</sub> values were 0.0282 (*I* > 2σ(*I*)) and 0.0289 (all data). The final *wR*(*F*<sup>2</sup>) values were 0.0711 (*I* > 2σ(*I*)) and 0.0718 (all data). The goodness of fit on *F*<sup>2</sup> was 1.045. CCDC no. CCDC 942342.

**Crystal data for 6:** C<sub>10</sub>H<sub>3</sub>BrCl<sub>2</sub>I<sub>2</sub>N<sub>2</sub>, *M* = 555.75, monoclinic, *a* = 26.6463(3) Å, *b* = 8.86220(10) Å, *c* = 13.57710(10) Å, β = 119.9080(10)°, *V* = 2779.19(5) Å<sup>3</sup>, *T* = 110(2) K, space group *C*2, *Z* = 8, μ(Mo *K*α) = 7.762 mm<sup>–1</sup>, 87960 reflections measured, 11433 independent reflections (*R*<sub>int</sub> = 0.0254). Flack parameter = –0.001(4). The final *R*<sub>1</sub> values were 0.0152 (*I* > 2σ(*I*)) and 0.0158 (all data). The final *wR*(*F*<sup>2</sup>) values were 0.0348 (*I* > 2σ(*I*)) and 0.0350 (all data). The goodness of fit on *F*<sup>2</sup> was 1.080. CCDC no. CCDC 942343.

**Crystal data for 7c:** C<sub>13</sub>H<sub>12</sub>Br<sub>2</sub>Cl<sub>2</sub>N<sub>2</sub>Si, *M* = 455.06, orthorhombic, *a* = 9.3313(1) Å, *b* = 13.9522(1) Å, *c* = 25.8239(1) Å, *V* = 3362.07(5) Å<sup>3</sup>, *T* = 110(2) K, space group *P*2<sub>1</sub>2<sub>1</sub>2<sub>1</sub>, *Z* = 8, μ(Cu *K*α) = 9.638 mm<sup>–1</sup>, 117489 reflections measured, 7061 independent reflections (*R*<sub>int</sub> = 0.0327). Flack parameter = 0.002(10). The final *R*<sub>1</sub> values were 0.0187 (*I* > 2σ(*I*)) and 0.0187 (all data). The final *wR*(*F*<sup>2</sup>) values were 0.0484 (*I* > 2σ(*I*)) and 0.0484 (all data). The goodness of fit on *F*<sup>2</sup> was 1.124. CCDC no. CCDC 942344.

**Crystal data for 7d:** C<sub>13</sub>H<sub>12</sub>Br<sub>2</sub>Cl<sub>2</sub>N<sub>2</sub>Sn, *M* = 545.66, orthorhombic, *a* = 9.36000(10) Å, *b* = 14.37080(10) Å, *c* = 26.1227(2) Å, *V* = 3513.78(5) Å<sup>3</sup>, *T* = 110(2) K, space group *P*2<sub>1</sub>2<sub>1</sub>2<sub>1</sub>, *Z* = 8, μ(Cu *K*α) = 19.641 mm<sup>–1</sup>, 33415 reflections measured, 7378 independent reflections (*R*<sub>int</sub> = 0.0359). Flack parameter = 0.002(4). The final *R*<sub>1</sub> values were 0.0302 (*I* > 2σ(*I*)) and 0.0303 (all data). The final *wR*(*F*<sup>2</sup>) values were 0.0795 (*I* > 2σ(*I*)) and 0.0796 (all data). The goodness of fit on *F*<sup>2</sup> was 1.071. CCDC no. CCDC 942345.

**Crystal data for 8a:** C<sub>16</sub>H<sub>9</sub>Br<sub>2</sub>Cl<sub>2</sub>N<sub>2</sub>, *M* = 458.96, orthorhombic, *a* = 8.6743(1) Å, *b* = 10.3483(1) Å, *c* = 17.3438(2) Å, *V* = 1556.85(3) Å<sup>3</sup>, *T* = 110(2) K, space group *P*2<sub>1</sub>2<sub>1</sub>2<sub>1</sub>, *Z* = 4, μ(Mo *K*α) = 5.544 mm<sup>–1</sup>, 24187 reflections measured, 4866 independent reflections (*R*<sub>int</sub> = 0.0182). Flack parameter = 0.000(4). The final *R*<sub>1</sub> values were 0.0152 (*I* > 2σ(*I*)) and 0.0159 (all data). The final *wR*(*F*<sup>2</sup>) values were 0.0363 (*I* > 2σ(*I*)) and 0.0366 (all data). The goodness of fit on *F*<sup>2</sup> was 1.070. CCDC no. CCDC 942346.

**Crystal data for 8d:**  $C_{15}H_7Br_2Cl_2N_3$ ,  $M = 459.96$ , orthorhombic,  $a = 8.4324(1) \text{ \AA}$ ,  $b = 10.3748(1) \text{ \AA}$ ,  $c = 17.2945(2) \text{ \AA}$ ,  $V = 1513.00(3) \text{ \AA}^3$ ,  $T = 110(2) \text{ K}$ , space group  $P2_12_12_1$ ,  $Z = 4$ ,  $\mu(\text{Cu K}\alpha) = 10.036 \text{ mm}^{-1}$ , 15483 reflections measured, 3173 independent reflections ( $R_{\text{int}} = 0.0316$ ). Flack parameter =  $-0.012(13)$ . The final  $R_1$  values were 0.0173 ( $I > 2\sigma(I)$ ) and 0.0175 (all data). The final  $wR(F^2)$  values were 0.0467 ( $I > 2\sigma(I)$ ) and 0.0467 (all data). The goodness of fit on  $F^2$  was 1.092. CCDC no. CCDC 942347.

**Crystal data for 9:**  $C_{18}H_8Br_2Cl_2N_2$ ,  $M = 482.98$ , monoclinic,  $a = 7.1636(1) \text{ \AA}$ ,  $b = 29.2923(2) \text{ \AA}$ ,  $c = 8.4859(1) \text{ \AA}$ ,  $\beta = 94.362(1)^\circ$ ,  $V = 1775.51(3) \text{ \AA}^3$ ,  $T = 110(2) \text{ K}$ , space group  $P2_1$ ,  $Z = 4$ ,  $\mu(\text{Cu K}\alpha) = 8.575 \text{ mm}^{-1}$ , 34991 reflections measured, 7421 independent reflections ( $R_{\text{int}} = 0.0249$ ). Flack parameter = 0.001(11). The final  $R_1$  values were 0.0325 ( $I > 2\sigma(I)$ ) and 0.0326 (all data). The final  $wR(F^2)$  values were 0.0814 ( $I > 2\sigma(I)$ ) and 0.0815 (all data). The goodness of fit on  $F^2$  was 1.064. CCDC no. CCDC 942348.

## ■ ASSOCIATED CONTENT

### ■ Supporting Information

$^1\text{H}$  and  $^{13}\text{C}$  spectra of all compounds; X-ray structures of (*P*)-2, (*P*)-6, (*M*)-7c, (*M*)-7d, (*M*)-8a, (*M*)-8d, and (*M*)-9; discussion on the absolute configuration assignment of compounds 7a,b,f. This material is of charge free of charge via the Internet at <http://pubs.acs.org>.

## ■ AUTHOR INFORMATION

### Corresponding Author

\*E-mail: victor.mamane@univ-lorraine.fr.

### Notes

The authors declare no competing financial interest.

## ■ ACKNOWLEDGMENTS

We gratefully acknowledge the CNRS and Université de Lorraine for financial support. The Service Commun de Diffraction des rayons X-Université de Lorraine is thanked for providing access to crystallographic facilities.

## ■ REFERENCES

- (1) Monk, P. M. S. *The Viologens: Physicochemical Properties, Synthesis and Applications of the Salts of 4,4'-Bipyridines*; Wiley: Chichester, 2001.
- (2) Paleos, C. M.; Tsiourvas, D. *Angew. Chem., Int. Ed. Engl.* **1995**, *34*, 1696–1711.
- (3) Meiners, C.; Valiyaveetil, S.; Enkelmann, V.; Müllen, K. *J. Mater. Chem.* **1997**, *7*, 2367–2374.
- (4) Abboud, M.; Mamane, V.; Aubert, E. *Beilstein J. Org. Chem.* **2012**, *8*, 253–258.
- (5) Kelly, T. R.; Lee, Y.-J.; Mears, R. J. *J. Org. Chem.* **1997**, *62*, 2774–2781.
- (6) Swahn, B.-M.; Xue, Y.; Arzel, E.; Kallin, E.; Magnus, A.; Plobeck, N.; Viklund, J. *Bioorg. Med. Chem. Lett.* **2006**, *16*, 1397–1401.
- (7) Stanetty, P.; Röhring, J.; Schnürch, M.; Mihovilovic, M. D. *Tetrahedron* **2006**, *62*, 2380–2387.
- (8) Biradha, K.; Sarkar, M.; Rajput, L. *Chem. Commun.* **2006**, 4169–4179.
- (9) MOFs issue. *Chem. Soc. Rev.* **2009**, *38*, 1201–1504.
- (10) Tanaka, K.; Muraoka, T.; Hirayama, D.; Ohnishi, A. *Chem. Commun.* **2012**, *48*, 8577–8579.
- (11) Liu, Y.; Xuan, W.; Cui, Y. *Adv. Mater.* **2010**, *22*, 4112–4135.
- (12) Ma, L.; Abney, C.; Lin, W. *Chem. Soc. Rev.* **2009**, *38*, 1248.
- (13) Bringmann, G.; Price Mortimer, A. P.; Keller, P. A.; Gresser, M. J.; Garner, J.; Breuning, M. *Angew. Chem., Int. Ed.* **2005**, *44*, 5384–5427.
- (14) Rang, A.; Engeser, M.; Maier, N. M.; Nieger, M.; Lindener, W.; Schalley, C. A. *Chem.—Eur. J.* **2008**, *14*, 3855–3859.
- (15) Mamane, V.; Aubert, E.; Peluso, P.; Cossu, S. *J. Org. Chem.* **2012**, *77*, 2579–2583.

(16) Peluso, P.; Mamane, V.; Aubert, E.; Cossu, S. *J. Chromatogr. A* **2012**, *1251*, 91–100.

(17) Mongin, F.; Quéguiner, G. *Tetrahedron* **2001**, *57*, 4059–5090.

(18) Pierrat, P.; Gros, P. C.; Fort, Y. *Synlett* **2004**, 2319–2322.

(19) Abboud, M.; Mamane, V.; Aubert, E.; Lecomte, C.; Fort, Y. *J. Org. Chem.* **2010**, *75*, 3224–3231.

(20) Jenkins, H. A.; Abeyskera, D.; Dickieb, D. A.; Clyburne, J. A. C. *J. Chem. Soc., Dalton Trans.* **2002**, 3919–3922.

(21) Han, H.; Zhao, W.; Song, J.; Li, C.; Wang, H. *J. Org. Chem.* **2013**, *78*, 2726–2730.

(22) Such deprotonation behavior of pyridyllithium species was already proposed to explain the formation of secondary products during the reaction of 2,6-dibromopyridine with *n*-BuLi. See: Cai, D.; Hughes, D. L.; Verhoeven, T. R. *Tetrahedron Lett.* **1996**, *37*, 2537–2540.

(23) Except for compound 7d.

(24) Chromatographic parameters: Chiralpak IA (250 × 4.6 mm, 5  $\mu\text{m}$ ), *n*-hexane/2-propanol 95:5 as mobile phase, flow rate 0.8 mL/min,  $T = 22^\circ\text{C}$ ,  $\alpha = 1.34$ ,  $R_s = 4.0$ . Starting from 500 mg of *rac*-2 (HPLC chemical purity 85%), the HPLC multimilligram recovery led to 194 mg of atropisomer (*P*)-2 (91% recovery) and 185 mg of atropisomer (*M*)-2 (87% recovery). To enhance throughput, the technique of overlapping injections was used.

(25) Flack, H. D.; Bernardinelli, G. *Chirality* **2008**, *20*, 684–690.